


Research Article

Quantum thermal engine with spin 1/2 system and geometric phases and interference obtained by unitary transformations of mixed states

*Y. Ben-Aryeh 

Physics Department, Technion-Israel Institute of Technology, Haifa, 32000, Israel
E-mail: *phr65yb@physics.technion.ac.il

Received 24 November 2023, Revised 14 February 2024, Accepted 24 March 2024

Abstract

Quantum Carnot engine whose working medium is a two-dimensional spin 1/2 system, with a time-dependent magnetic field in the symmetric z direction is described. The dynamic of this engine is obtained by using four steps, where in two steps the system is coupled alternatively to hot and cold heat baths, and in the other two steps the time development is adiabatic and isentropic (with constant entropy). The conditions for getting a reversible Carnot cycle and the role of time duration for its irreversibility are discussed. Since the calculations are made for the expectation values of the Hamiltonian, only dynamical phases are obtained which cannot be used for interference effects. An alternative method is developed for getting geometric phases, which can be used in interferometry. Parallel transport equations for pure states are generalized to mixed states by which dynamical phases are eliminated. The geometric phases are derived by unitary SU(2) transformations, including time-dependent parameters which are a function of the magnetic fields interactions. A special form of the unitary transformation for the mixed thermal states is developed, by which geometric phases are obtained, which are different from those obtained in NMR and neutron interferometry.

Keywords: *Quantum thermodynamics; quantum heat engine; carnot cycle; geometric phases.*

1. Introduction

Quantum thermal engines connected to hot and cold heat baths have been studied extensively in various forms. The studies of such engines are based on Otto [1-4], Carnot, and other engines [5-8] cycles. While quantum properties of time dependent cycles were studied extensively, those studies emphasized the efficiency of such engines. In the present work, we raise the question of whether and how geometric and dynamical phases are involved in such cycles. This question is of much importance as the use of quantum phases in interference experiments may lead to important conclusions about the quantum or classical nature of such systems. The differences between dynamical and geometrical phases are described by following conventional theories [9-11].

A quantum Carnot engine is described, whose working medium is a two-dimensional spin 1/2 system with time dependent magnetic field in the symmetric z direction [6,7]. The dynamic of this engine is obtained by using four steps, where in two steps the system is coupled alternatively to hot and cold heat baths, and in the other two steps the time development is adiabatic and isentropic (with constant entropy). The conditions for getting a reversible Carnot cycle, and the role of time duration for its irreversibility are discussed. Since the calculations are made for the expectation of the Hamiltonian, only dynamical phases are obtained which cannot be used for interference effects. We use an alternative method for getting geometric phases which can be used in interferometry [12-15]. Parallel transport equations for pure states are generalized to mixed states by

which the dynamical phases are eliminated. The geometric phase is derived by unitary SU(2) transformations, including time-dependent parameters which are a function of the magnetic field interactions. We get a special form of the unitary transformation of the mixed thermal states by which geometric phases are obtained, which are different from those obtained in NMR and neutron interferometry.

The magnetic field \vec{B} is along the positive z axis and the Hamiltonian is given by:

$$\begin{aligned}\hat{H}(t) &= 2\mu_B B_z(t)\hat{s}_z \equiv \tilde{\omega}(t)\hat{s}_z; \\ \tilde{\omega}(t) &= 2\mu_B B_z(t).\end{aligned}\quad (1)$$

The units are such that $\hbar = 1$, μ_B is the Bohr magneton, $\tilde{\omega}(t)$ is proportional to $B_z(t)$ and \hat{s}_z is the spin operator in the z direction. We refer to $\tilde{\omega}(t)$ rather than $B_z(t)$ as “the field”. The mixed density matrix ρ_0 of this system is given by:

$$\rho_0 = P_1 | -1/2 \rangle \langle -1/2 | + P_2 | +1/2 \rangle \langle +1/2 |, \quad (2)$$

where $\{-1/2, +1/2\}$ are the eigenvalues of the spin and the classical probabilities P_1 and P_2 are given, respectively, by statistical mechanics as:

$$\begin{aligned}P_1 &= \frac{e^{\hbar\tilde{\omega}\beta/2}}{e^{\hbar\tilde{\omega}\beta/2} + e^{-\hbar\tilde{\omega}\beta/2}}; \quad P_2 = \frac{e^{-\hbar\tilde{\omega}\beta/2}}{e^{\hbar\tilde{\omega}\beta/2} + e^{-\hbar\tilde{\omega}\beta/2}}; \\ \beta &= \frac{1}{k_B T}\end{aligned}\quad (3)$$

where k_B is the Boltzmann constant, T the absolute temperature, μ_B is the Bohr magneton and $\tilde{\omega}$ was defined in Eq. (1). Based on statistical mechanics, the expectation value of \hat{s}_z is given by:

$$\langle s_z \rangle = -\frac{1}{2} \tanh(\tilde{\omega}\beta/2); \quad \beta = \frac{1}{k_B T}, \quad (4)$$

and the expectation value of the Hamiltonian is given by:

$$E_0 = \langle H_0 \rangle = \hbar \tilde{\omega} \langle s_z \rangle. \quad (5)$$

H_0 is the zero order Hamiltonian and E_0 is its expectation value.

Such a quantum machine works by different steps in which the energy of the spin 1/2 (considered as the working medium) is given by the expectation value of Eq. (5). In each step the temperature or the “frequency” $\tilde{\omega} = 2\mu_B B_z$ (or both parameters) are changing. In an alternative approach, we incorporate the geometric phase for mixed states interferometry [12] into the present thermal mixed systems using a general propagator. This two-dimensional spin system is different from the common examples of three-dimensional spin systems described in the Bloch sphere [13].

In the present article, I develop a method by which geometric phases can be obtained in quantum thermal engine systems, leading to interference effects in such systems. This method is applied in my work to a quantum Carnot engine whose working medium is a two-dimensional spin 1/2 system, with a time-dependent magnetic field in the symmetric z axis. Since the general calculations for quantum heat engines, and especially those made in my work for the present quantum system, are made with dynamical phases they do not lead to interference effects. I show by using special unitary transformations of mixed states, which are developed for the present Carnot cycle, the way by which geometric phases are produced. The possibility to obtain geometric phases has not been realized, so far, in the published literature on quantum heat engines. Realization of interference effects by geometric phases for quantum engines can give a new insight into quantum thermodynamics.

The present paper is arranged as follows: In section 2 we obtain the dynamical phases in the present spin 1/2 Carnot quantum engine. The efficiency of such engines under reversible and irreversible conditions is described. In section 3, we apply the geometric phases approach to mixed states as propagators of the quantum engines' thermal states. Results are summarized in Section 4.

2. Methods for reversible and irreversible Carnot cycle with spin 1/2 system

The Carnot engine including its efficiency can be analyzed under different limiting cases. In case A we assume that the parameters of the Carnot cycle are changed infinitely slowly along some path from a certain initial point to a final point. In this case, the Carnot quantum engine is reversible with maximal efficiency, but power is tending to zero. In case B we treat the irreversible Carnot cycle, which gives maximal power but with energy losses. We show in the

following analysis that there is a trade between maximum power, and maximum efficiency at which power is zero.

Case A: Reversible Carnot cycle

Carnot quantum engine operates by 4 steps described schematically in Figure 1.

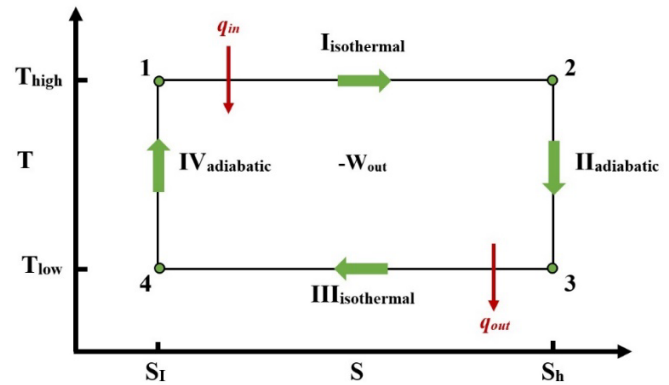


Figure 1. Carnot cycle is described, where the 4 points 1, 2, 3, and 4 denote 4 different states of the system. The transitions between states 1 and 2, and that between states 3 and 4 are described, for the hot isotherm at the temperature T_{high} , and for the cold isotherm at the temperature T_{low} , respectively. The transitions between states 2 and 3, and that between states 4 and 1 are adiabatic with constant entropy S_h and S_l , respectively.

In each of the points 1, 2, 3, and 4 the expectation value of the Hamiltonian of Eq. (5) is given as $\hbar \tilde{\omega} \langle s_z \rangle$ where $\tilde{\omega}(t) = 2\mu_B B_z(t)$, and $\langle s_z \rangle = -(1/2) \tanh(\tilde{\omega}\beta/2)$ is the expectation value of the spin 1/2 \hat{s}_z operator. In the transitions between consecutive points, the parameter $\tilde{\omega}$ (proportional to the magnetic field) or $\beta = 1/k_B T$ (or both) are changing. The transition between points 1 and 2 describes the hot isotherm (see Fig. 1 as $I_{isothermal}$), where the system is coupled to a hot reservoir at temperature T_{high} . In this step, heat q_{in} is entering into the system. The transition between points 3 and 4 describes the cold isotherm (see Fig. 1 as $III_{isothermal}$), where the system is coupled with the cold reservoir with temperature T_{low} . At this step, heat q_{out} is going out of the system. The transitions between points 2 and 3 are adiabatic and isentropic (described in Fig. 1 as $II_{adiabatic}$ with constant entropy S_h). The transitions between 4 and 1 are adiabatic and isentropic (described in Fig. 1 as $IV_{adiabatic}$ with constant entropy S_l). In these steps (denoted as $II_{adiabatic}$ and $IV_{adiabatic}$), heat is not transferred as the system is isolated from the reservoirs, but work is done by decreasing or increasing the temperature by the difference $\pm(T_H - T_C)$, respectively. For an ideal Carnot cycle (assuming no losses) the work done by such a thermal machine is given by $q_{in} + q_{out}$ where q_{out} is negative, and its efficiency is given by the limit $\eta = (q_{in} + q_{out})/q_{in} = (T_{high} - T_{low})/T_{high}$.

The schematic Fig. 1 describes only the physical nature of the present Carnot cycle, but it does not describe quantitatively the experimental values in these steps. Explicit evaluations of the experimental values of the present quantum Carnot engine can be given as follows.

The heat q_{in} by the present spin system is positive and given by:

$$\begin{aligned}
q_{in} &= \langle H_2 \rangle - \langle H_1 \rangle = \\
&= \frac{\hbar}{2} [-\tilde{\omega}_2 \tanh(\beta_H \hbar \tilde{\omega}_2) + \tilde{\omega}_1 \tanh(\beta_H \hbar \tilde{\omega}_1)]; \\
\beta_H &= 1/k_B T_{high}; \quad \tilde{\omega}_1 = 2\mu_B B_z(1); \\
\tilde{\omega}_2 &= 2\mu_B B_z(2); \quad \tilde{\omega}_1 > \tilde{\omega}_2
\end{aligned} \tag{6}$$

The heat q_{out} of the present spin system is negative and given by:

$$\begin{aligned}
q_{out} &= \langle H_4 \rangle - \langle H_3 \rangle = \\
&= \frac{\hbar}{2} [-\tilde{\omega}_4 \tanh(\beta_C \hbar \tilde{\omega}_4) + \tilde{\omega}_3 \tanh(\beta_C \hbar \tilde{\omega}_3)]; \\
\beta_C &= 1/k_B T_{low}; \quad \tilde{\omega}_3 = 2\mu_B B_z(3); \\
\tilde{\omega}_4 &= 2\mu_B B_z(4); \quad \tilde{\omega}_4 > \tilde{\omega}_3.
\end{aligned} \tag{7}$$

We find by the above equations that while q_{in} is positive q_{out} is negative. Since in the adiabatic transitions between states 2 and 3, and that between states 4 and 1, the entropy is not changed (isentropic transitions), the probabilities P_1 and P_2 are also not changed (as $P_1 + P_2 = 1$ in our system). It follows from Eq. (4) that the expectation value $\langle s_z \rangle = -(1/2) \tanh(\hbar \omega \beta / 2)$ is also constant in these transitions. Using these relations, we get:

$$\begin{aligned}
\beta_H \tilde{\omega}_1 &= \beta_C \tilde{\omega}_4; \quad \beta_H \tilde{\omega}_2 = \beta_C \tilde{\omega}_3; \\
\frac{\tilde{\omega}_4}{\tilde{\omega}_1} &= \frac{\tilde{\omega}_3}{\tilde{\omega}_2} = \frac{\beta_H}{\beta_C} = \frac{T_{low}}{T_{high}}.
\end{aligned} \tag{8}$$

Substituting Eqs. (8) into those of (6) and (7) we get the efficiency of the Carnot reversible cycle as:

$$\eta_{rev} = \frac{q_{in} + q_{out}}{q_{in}} = 1 - \frac{T_{low}}{T_{high}}. \tag{9}$$

Case B: Irreversible Carnot cycle

There are various works treating the irreversibility of the Carnot cycle. We refer here to [5] where a simple model (without entering into the detailed interactions) was developed which gives fair comparisons with experimental results under different conditions. We use here the idea that the irreversible heat from the cold (hot) reservoir will decay with time τ_C (τ_H) as:

$$\begin{aligned}
Q_{ir,C} &= T_{low} \left(-\Delta S - \frac{C_1}{\tau_C} \right); \\
Q_{ir,H} &= T_{high} \left(\Delta S - \frac{C_2}{\tau_H} \right).
\end{aligned} \tag{10}$$

Here ΔS represents the entropy difference $S_h - S_l$, the subscripts H and C refer to the hot and cold reservoir, respectively, C_1 and C_2 are certain constants τ_C and τ_H are decay times and the subscript ir represents irreversibility (the reversible regime is approached in times $\tau_C \rightarrow \infty$, $\tau_H \rightarrow \infty$). We consider the power generated during the Carnot cycle and by using Eq. (10) we get:

$$\begin{aligned}
P &= \frac{-W_{out}}{\tau_H + \tau_C} = \\
&= \frac{(T_{high} - T_{low}) \Delta S - T_{low} (C_1 / \tau_C) - T_{high} (C_2 / \tau_H)}{\tau_H + \tau_C},
\end{aligned} \tag{11}$$

where for $-W_{out}$ described in Fig. 1, we inserted the decay times as given by Eq. (11).

The maximum power is found by setting the derivatives of P with respect to τ_H and τ_C equal to zeros. Such a procedure was developed in [5], obtaining different results including the case $C_1 = C_2$ for which Curzon-Ahlborn efficiency [8] was obtained.

There are many other works treating the effects of energy losses on quantum engines' efficiency, but our interest in the present paper is about the possibility to use geometric phases in quantum engines. Since the dynamical phases obtained above for Carnot engine (and similar dynamical phases which can be obtained for other engines) are based on expectation values of the Hamiltonian, they cannot be used for interference experiments. We show in the next section an alternative approach by which geometric phases can be obtained for thermal states which can be applied in interferometers, e.g., in Mach-Zehnder interferometer [12]. The geometric phases obtained for thermal states are different from those obtained in NMR and Neutron interferometry [16-19].

3. Results for geometric phases applied to thermal spin 1/2 states

The density matrix ρ_0 for mixed states includes averaging of thermal fluctuations described by the probabilities P_k . Therefore, unitary transformations cannot operate directly on this density matrix, but they can operate separately on the components of such density matrix composed of pure quantum states. The idea presented in [12] is that the initial density matrix ρ_0 can be developed in time t to a density matrix ρ_t by the unitary transformation operating on the initial vectors $|\tilde{k}\rangle_0$ as:

$$\rho_t = \sum_{k=1}^N P_k \left\{ U(t) |\tilde{k}\rangle_0 \langle \tilde{k}|_0 U^\dagger(t) \right\} = \sum_{k=1}^N P_k |\tilde{k}\rangle_t \langle \tilde{k}|_t \tag{12}$$

where $U(t)$ is a unitary matrix of $N \times N$ dimension, $|\tilde{k}\rangle_t = U(t) |\tilde{k}\rangle_0$ are the orthonormal vectors at time t and $|\tilde{k}\rangle_0$ are the initial vectors. The mixed state is described as a mixture of several pure states incoherently weighed by their respective probabilities P_k . For thermal states the eigenvectors in the computational basis are given by:

$$|\tilde{1}\rangle_0 = \begin{pmatrix} 1 \\ 0 \end{pmatrix}; |\tilde{2}\rangle_0 = \begin{pmatrix} 0 \\ 1 \end{pmatrix}. \tag{13}$$

corresponding to eigenvalues $-1/2$ and $+1/2$ of \hat{s}_z . The density matrix of Eq. (2) is transformed to short notation as:

$$\begin{aligned}
\rho_0 &= P_1 |-1/2\rangle \langle -1/2| + P_2 |+1/2\rangle \langle +1/2| = \\
&= P_1 |\tilde{1}\rangle \langle \tilde{1}| + P_2 |\tilde{2}\rangle \langle \tilde{2}|.
\end{aligned} \tag{14}$$

The parallel transport of a particular vector $|\tilde{k}\rangle_t$ implies no change in phase when $|\tilde{k}\rangle_t$ evolves into $|\tilde{k}\rangle_{t+dt}$, for some infinitesimal change of the parameter t . Although locally there is no phase change, the system can acquire a geometric phase after completing a closed loop parametrized by t or by the Pancharatnam phase for open cycle. This phase is related to curvature of the parameter space depending only on the geometry of the path. Parallel transport can be satisfied by choosing a suitable $U(t)$ matrix which satisfies the parallel transport conditions, where for the present 1/2 spin system we have such two equations.

The geometric phase γ_{geom} is acquired by a mixed state evolving along a curve Γ under a unitary transformation which satisfies the parallel transport equations and is given by:

$$\begin{aligned}\gamma_{geom}(\Gamma) &= \arg \text{Tr}[\rho_t U(t)] = \\ &= \arg \text{Tr}[U(t) \rho_0 U^\dagger(t) U(t)] = \arg \text{Tr}[U(t) \rho_0].\end{aligned}\quad (15)$$

$U(t)$ for thermal states is given by SU(2), a two-dimensional unitary matrix. We choose $U(t)$ to be given by the product of 3 unitary matrices:

$$U(t) = U_1(\tilde{\omega}_1) U_2(\xi) U_3(\tilde{\omega}_2), \quad (16)$$

$$\begin{aligned}U_1(\tilde{\omega}_1) &= \begin{bmatrix} \exp[i\tilde{\omega}_1 t / 2 + \phi] & 0 \\ 0 & \exp[-i\tilde{\omega}_1 t / 2 + \phi] \end{bmatrix}; \\ U_3(\tilde{\omega}_2) &= \begin{bmatrix} \exp[i\tilde{\omega}_2 t / 2] & 0 \\ 0 & \exp[-i\tilde{\omega}_2 t / 2] \end{bmatrix}\end{aligned}\quad (17)$$

and

$$U_2(\xi) = \begin{bmatrix} \cos \xi & -\sin \xi \\ \sin \xi & \cos \xi \end{bmatrix}. \quad (18)$$

We assume here that $U_1(\tilde{\omega}_1)$ and $U_3(\tilde{\omega}_2)$ operate during time t with Hamiltonians fixed by Eq. (1) as $H_{1z} = \hbar \tilde{\omega}_1 \sigma_z / 2$ and $H_{2z} = \hbar \tilde{\omega}_2 \sigma_z / 2$ respectively, where $\tilde{\omega}_1 = 2\mu_B B_{1z}$ and $\tilde{\omega}_2 = 2\mu_B B_{2z}$, B_{1z} and B_{2z} are constant magnetic fields in the z direction and where ϕ is a certain phase shift between $U_1(\tilde{\omega}_1)$ and $U_3(\tilde{\omega}_2)$. $U_2(\xi)$ is a simple beam-splitter transformation which does not include any time dependence and for simplicity is defined by Eq. (18).

By substituting Eqs. (17-18) into that of (16) we get:

$$U(t) = e^{i\phi} \begin{pmatrix} e^{i\delta t} \cos \xi & -e^{-i\zeta t} \sin \xi \\ e^{i\zeta t} \sin \xi & e^{-i\delta t} \cos \xi \end{pmatrix} \quad (19)$$

$$\delta = \frac{\tilde{\omega}_1 + \tilde{\omega}_2}{2} \quad ; \quad \zeta = \frac{\tilde{\omega}_2 - \tilde{\omega}_1}{2}. \quad (20)$$

Equation (19) is similar to the SU(2) transformation used in neutron interferometry [19]. But here the parameters δ and ζ are multiplied by the time t which leads to a certain dependence of U on time, which is critical for the use of the following analysis.

Realization of the above unitary transformation depends on scales of time. The initial mixed state of Eqs. (2-3) can be produced after a relatively long time in which the system arrives at thermal equilibrium. The operation of the unitary transformation on the initial state is made during time t which is short relative to relaxation times.

We use the above $U(t)$ unitary matrix for obtaining parallel transport equations. Due to the linear relations between $|\tilde{k}\rangle_t$ and $|\tilde{k}\rangle_0$ the two parallel transport equations $\langle \tilde{k}_t | U(t) U^\dagger(t) | \tilde{k}_t \rangle = 0$ ($k=1,2$) implies also:

$$\langle \tilde{k}_0 | U(t) U^\dagger(t) | \tilde{k}_0 \rangle = 0 \quad ; \quad k=1,2. \quad (21)$$

We use the eigenvectors of $|\tilde{k}\rangle_0$ in the computational basis given by Eqs. (13). Then we get by using the first Eq. of (21) and that of (19) for

$$\begin{aligned}(1,0) & \begin{pmatrix} (i\delta \cos \xi) e^{i\delta t} & (i\zeta \sin \xi) e^{-i\zeta t} \\ (i\zeta \sin \xi) e^{i\zeta t} & (-i\delta \cos \xi) e^{-i\delta t} \end{pmatrix} \\ & \times \begin{pmatrix} \cos \xi e^{-i\delta t} & \sin \xi e^{-i\zeta t} \\ -\sin \xi e^{i\zeta t} & \cos \xi e^{i\delta t} \end{pmatrix} \begin{pmatrix} 1 \\ 0 \end{pmatrix} = 0\end{aligned}\quad (22)$$

Straightforward calculations lead to the result:

$$\begin{aligned}& \begin{pmatrix} (i\delta \cos \xi) e^{i\delta t} & (i\zeta \sin \xi) e^{-i\zeta t} \\ \cos \xi e^{-i\delta t} & \sin \xi e^{-i\zeta t} \\ -\sin \xi e^{i\zeta t} & \cos \xi e^{i\delta t} \end{pmatrix} = i\delta (\cos \xi)^2 - i\zeta (\sin \xi)^2 = 0\end{aligned}\quad (23)$$

For the second equation of (21) we use calculations from equation (22) in which we exchange $\begin{pmatrix} 1 & 0 \end{pmatrix}$ to $\begin{pmatrix} 0 & 1 \end{pmatrix}$ and

$$\begin{pmatrix} 1 \\ 0 \end{pmatrix} \text{ to } \begin{pmatrix} 0 \\ 1 \end{pmatrix}.$$

Then we get:

$$\begin{aligned}& \begin{pmatrix} i\zeta \sin \xi e^{i\zeta t} & -i\delta \cos \xi e^{-i\delta t} \\ e^{-i\zeta t} \sin \xi & e^{i\delta t} \cos \xi \end{pmatrix} = i\zeta (\sin \xi)^2 - i\delta (\cos \xi)^2 = 0.\end{aligned}\quad (24)$$

The equivalent equations (23) and (24) lead to a sufficient condition for parallel transport:

$$\begin{aligned}(\tan \xi)^2 &= \frac{\delta}{\zeta}; \\ \cos^2 \xi \left(1 + \frac{\delta^2}{\zeta^2} \right) &= 1 \rightarrow \cos \xi = \sqrt{\frac{\zeta^2}{\delta^2 + \zeta^2}}\end{aligned}\quad (25)$$

Using Eq. (13), and that of (16) for $U(t)$ we get:

$$\begin{aligned}\langle 1|_0 U(t) |1\rangle_0 &= \cos \xi e^{i(\delta t + \phi)}; \\ \langle 2|_0 U(t) |2\rangle_0 &= \cos \xi e^{-i(\delta t + \phi)}.\end{aligned}\quad (26)$$

The geometric phase γ_{geom} is obtained by the incoherent superposition of two fields produced separately from the two components of the thermal field so that it is given by:

$$\gamma_{geom} = \arg \left[P_1 \cos \xi e^{i(\delta t + \phi)} + P_2 \cos \xi e^{-i(\delta t + \phi)} \right] \quad (27)$$

From Eq. (27) we get the result:

$$\gamma_{geom} = \arctan \left[\left(\frac{P_1 - P_2}{P_1 + P_2} \right) \tan(\delta t + \phi) \right], \quad (28)$$

where for the present system $P_1 + P_2 = 1$. Radiation intensity is reduced by the factor:

$$\tilde{\nu} = \left| P_1 \cos \xi e^{i(\delta t + \phi)} + P_2 \cos \xi e^{-i(\delta t + \phi)} \right| = \cos \xi \sqrt{P_1^2 + P_2^2 + 2P_1 P_2 \cos(2\delta t + 2\phi)}. \quad (29)$$

The unitary development of the spin 1/2 system was produced by the consecutive interactions of this system with magnetic fields in times which are short relative to relaxation times in this system. Parallel transport equations, which eliminate the dynamical phase, were obtained by assuming the relations of Eq. (25) between the parameters included in the analysis. For the present mixed spin 1/2 system $\delta t + \phi$ represents the Pancharatnam's phase for open cycle and $(P_1 - P_2)/(P_1 + P_2)$ represents the thermal noise parameter.

By using equation (3) the thermal noise term can be transformed to:

$$\left(\frac{P_1 - P_2}{P_1 + P_2} \right) = \tanh \left[\frac{\hbar \tilde{\omega} \beta}{2} \right]. \quad (30)$$

For very low temperatures this term tends to the value 1. For very high temperatures we can use the approximations:

$$\sinh \left[\frac{\hbar \tilde{\omega} \beta}{2} \right] = \frac{\hbar \tilde{\omega} \beta}{2}; \quad \cosh \left[\frac{\hbar \tilde{\omega} \beta}{2} \right] = 1; \quad (31)$$

$$\left(\frac{P_1 - P_2}{P_1 + P_2} \right) = \frac{\hbar \tilde{\omega}}{2k_B T}$$

so that this term is given by the ratio between the quantum vacuum energy $\hbar \tilde{\omega}/2$ and the thermal energy $k_B T$. It is interesting to note that the Pancharatnam phase for open cycle in neutrons experiments [19] was obtained for open cycles.

4. Conclusions

The efficiency of thermal engines and the role of time durations for getting maximum efficiency was analyzed. Two-dimensional Carnot thermal spin 1/2 system with time-dependent magnetic fields in the symmetric z was analyzed. The density matrix ρ_0 obtained for mixed states includes averaging of thermal fluctuations with the probability $P_k (k=1,2)$ and therefore it cannot be used in interferometry. The use of unitary transformation of mixed states, including the parallel transport equations to these states, were found to be of special interest, as by their use

dynamical phases are eliminated and we remain with geometric phases. We find that the geometric phases obtained by the unitary transformation are Pancharatnam's phases which are gauge invariant and are valid also for open circles. It is interesting to find that geometric phases can be obtained in quantum engine systems, which lead to interference effects, and which are different from the common ones in NMR and neutron interferometry. In conclusion, geometric phases which can be obtained in quantum engines (and which were not observed so far) will lead to new insights in quantum thermodynamics.

Acknowledgements

The present study was supported by Technion-Mossad under grant No. 2007156.

Conflict of interest

The author declares no conflicts of interest, Artificial AI-assisted technology was not used.

Role of the Corresponding Author

The article was obtained by Y. Ben-Aryeh investigation.

References:

- [1] R. Kosloff and Y. Rezek, "The Quantum Harmonic Otto Cycle," *Entropy*, vol. 19, no. 4, p. 136, Mar. 2017, doi: 10.3390/e19040136.
- [2] H. S. Leff, "Thermal efficiency at maximum work output: New results for old heat engines," *Am J Phys*, vol. 55, no. 7, pp. 602–610, Jul. 1987, doi: 10.1119/1.15071.
- [3] J. Roßnagel *et al.*, "A single-atom heat engine," *Science* (1979), vol. 352, no. 6283, pp. 325–329, Apr. 2016, doi: 10.1126/science.aad6320.
- [4] O. Abah *et al.*, "Single-Ion Heat Engine at Maximum Power," *Phys Rev Lett*, vol. 109, no. 20, p. 203006, Nov. 2012, doi: 10.1103/PhysRevLett.109.203006.
- [5] M. Esposito, R. Kawai, K. Lindenberg, and C. Van den Broeck, "Efficiency at Maximum Power of Low-Dissipation Carnot Engines," *Phys Rev Lett*, vol. 105, no. 15, Oct. 2010, Art. no. 150603, doi: 10.1103/PhysRevLett.105.150603.
- [6] E. Geva and R. Kosloff, "A quantum-mechanical heat engine operating in finite time. A model consisting of spin-1/2 systems as the working fluid," *J Chem Phys*, vol. 96, no. 4, pp. 3054–3067, Feb. 1992, doi: 10.1063/1.461951.
- [7] B. Lin and J. Chen, "Optimal analysis of the performance of an irreversible quantum heat engine with spin systems," *J Phys A Math Gen*, vol. 38, no. 1, pp. 69–79, Jan. 2005, doi: 10.1088/0305-4470/38/1/004.
- [8] F. L. Curzon and B. Ahlborn, "Efficiency of a Carnot engine at maximum power output," *Am J Phys*, vol. 43, no. 1, pp. 22–24, Jan. 1975, doi: 10.1119/1.10023.
- [9] M. V. Berry, "Quantal phase factors accompanying adiabatic changes," *Proceedings of the Royal Society of London. A. Mathematical and Physical Sciences*, vol. 392, no. 1802, pp. 45–57, Mar. 1984, doi: 10.1098/rspa.1984.0023.

- [10] Y. Ben-Aryeh, “Berry and Pancharatnam topological phases of atomic and optical systems,” *Journal of Optics B: Quantum and Semiclassical Optics*, vol. 6, no. 4, pp. R1–R18, Apr. 2004, doi: 10.1088/1464-4266/6/4/R01.
- [11] Y. Aharonov and J. Anandan, “Phase change during a cyclic quantum evolution,” *Phys Rev Lett*, vol. 58, no. 16, pp. 1593–1596, Apr. 1987, doi: 10.1103/PhysRevLett.58.1593.
- [12] E. Sjöqvist *et al.*, “Geometric Phases for Mixed States in Interferometry,” *Phys Rev Lett*, vol. 85, no. 14, pp. 2845–2849, Oct. 2000, doi: 10.1103/PhysRevLett.85.2845.
- [13] E. Sjöqvist, “Quantal phase in split-beam interferometry,” *Phys Rev A (Coll Park)*, vol. 63, no. 3, Feb. 2001, Art. no. 035602, doi: 10.1103/PhysRevA.63.035602.
- [14] S. Pancharatnam, “Generalized theory of interference, and its applications,” *Proceedings of the Indian Academy of Sciences - Section A*, vol. 44, no. 5, pp. 247–262, Nov. 1956, doi: 10.1007/BF03046050.
- [15] A. G. Wagh and V. C. Rakhecha, “On measuring the Pancharatnam phase. I. Interferometry,” *Phys Lett A*, vol. 197, no. 2, pp. 107–111, Jan. 1995, doi: 10.1016/0375-9601(94)00914-B.
- [16] Ghosh and A. Kumar, “Experimental measurement of mixed state geometric phase by quantum interferometry using NMR,” *Phys Lett A*, vol. 349, no. 1–4, pp. 27–36, Jan. 2006, doi: 10.1016/j.physleta.2005.08.092.
- [17] M. Ericsson, D. Achilles, J. T. Barreiro, D. Branning, N. A. Peters, and P. G. Kwiat, “Measurement of Geometric Phase for Mixed States Using Single Photon Interferometry,” *Phys Rev Lett*, vol. 94, no. 5, Feb. 2005, Art. no. 050401, doi: 10.1103/PhysRevLett.94.050401.
- [18] J. Du *et al.*, “Observation of Geometric Phases for Mixed States using NMR Interferometry,” *Phys Rev Lett*, vol. 91, no. 10, Sep. 2003, Art. no. 100403, doi: 10.1103/PhysRevLett.91.100403.
- [19] J. Klepp, S. Sponar, Y. Hasegawa, E. Jericha, and G. Badurek, “Noncyclic Pancharatnam phase for mixed state evolution in neutron polarimetry,” *Phys Lett A*, vol. 342, no. 1–2, pp. 48–52, Jul. 2005, doi: 10.1016/j.physleta.2005.05.038.